THE UNIVERSITY OF CHICAGO

THE MAXIMUM ENERGY OF SHOCK-ACCELERATED COSMIC RAYS

A DISSERTATION SUBMITTED TO
THE FACULTY OF THE PHYSICAL SCIENCES DIVISION
IN CANDIDACY FOR THE DEGREE OF
DOCTOR OF PHILOSOPHY

BY
REBECCA RIMAI DIESING

CHICAGO, ILLINOIS
AUGUST 2023

Table of Contents

List of Figures

This thesis represents the motivations, results, and conclusions from the following single-author paper:

[3] *The Maximum Energy of Shock-Accelerated Cosmic Rays*. R. Diesing, submitted to The Astrophysical Journal.

Abstract

Identifying the accelerators of Galactic cosmic ray protons (CRs) with energies up to a few PeV (10^{15} eV) remains a theoretical and observational challenge. Supernova remnants (SNRs) represent strong candidates, as they provide sufficient energetics to reproduce the CR flux observed at Earth. However, it remains unclear whether they can accelerate particles to PeV energies, particularly after the very early stages of their evolution. This uncertainty has prompted searches for other source classes and necessitates comprehensive theoretical modeling of the maximum proton energy, $E_{\rm max}$, accelerated by an arbitrary shock. While analytic estimates of $E_{\rm max}$ have been put forward in the literature, they do not fully account for the complex interplay between particle acceleration, magnetic field amplification, and shock evolution. This paper uses a multi-zone, semi-analytic model of particle acceleration based on kinetic simulations to place constraints on $E_{\rm max}$ for a wide range of astrophysical shocks. In particular, we develop relationships between $E_{\rm max}$, shock velocity, size, and ambient medium. We find that SNRs can only accelerate PeV particles under a select set of circumstances, namely, if the shock velocity exceeds $\sim 10^4$ km s^{-1} and escaping particles drive magnetic field amplification. However, older, slower SNRs may still produce observational signatures of PeV particles due to populations accelerated when the shock was younger. Our results serve as a reference for modelers seeking to quickly produce a self-consistent estimate of the maximum energy accelerated by an arbitrary astrophysical shock.

Chapter 1

Introduction

After more than a century of study, the origins of the cosmic rays (CRs) detected on Earth remain uncertain. In the case of Galactic CRs, with energies up to a few PeV (10^{15} eV), supernova remnants (SNRs) remain promising candidates, as they provide sufficient energetics and an efficient acceleration mechanism [4–7]. Moreover, there is strong observational evidence that SNRs are capable particle accelerators, including the detection of hadronic γ-ray emission produced by collisions between CR protons and protons in the interstellar medium (ISM) [e.g., 8–10].

In the standard paradigm, CRs are accelerated at the forward shocks of SNRs via *diffusive shock accelration* (DSA). In this picture, particles scatter off of magnetic perturbations such that they diffuse back and forth across the shock, gaining energy with each crossing [11–15]. This mechanism produces power-law distributions of particles and is capable of accelerating particles up to arbitrarily high energies, provided that they remain confined close to the shock. Moreover, DSA represents a universal mechanism that can explain particle acceleration in a multitude of astrophysical contexts [e.g., 16, 17].

However, it is unclear whether SNRs confine CRs long enough to accelerate them up to the so-called "knee", a feature in the CR proton spectrum around a few PeV [e.g., 18–20] and the presumed maximum energy of Galactic CR protons. Namely, in the absence of

strong magnetic field amplification, SNRs are unable to confine PeV particles [21]. While there is clear theoretical [e.g., 22–25] and observational [e.g., 26–30] evidence that particle acceleration can drive strong magnetic field amplification in SNRs, the question of whether that amplification is sufficient to confine PeV particles remains contested in the literature [e.g., 1, 6, 31–36].

Observational efforts to search for PeVatrons have also called into question the SNR paradigm for Galactic CR acceleration. While $\gtrsim 100$ TeV γ-ray sources have been detected with instruments such as the Large High Altitude Air Shower Observatory (LHAASO) [37], the High Altitude Water Cherenkov Observatory (HAWC) [38], and the High Energy Stereoscopic System (H.E.S.S.) [39], many of these sources do not appear to coincide with known SNRs. These results motivate the search for alternative sources of PeV protons, such as pulsar winds [e.g., 40], microquasars [e.g., 41], star clusters [e.g., 42, 43], and superbubbles [e.g., 44]. Notably, these alternative PeVatron candidates often still involve shocks, and tend to invoke DSA as the predominant acceleration mechanism.

In this paper, we place constraints on the maximum proton energy, $E_{\rm max}$, accelerated by an arbitrary astrophysical shock using a self-consistent, multi-zone model for particle acceleration and magnetic field amplification. While we tailor our model parameters to SNRs in order to analyze their potential to be PeVatrons, we also develop scaling relations that can be applied to any spherical shock. We also cast these scaling relations in terms of parameters that can be inferred observationally (e.g., shock velocity). Finally, we bracket theoretical uncertainties in the nature of magnetic field amplification, resulting in robust lower and upper limits on $E_{\rm max}$. This combination of features—our multi-zone, self-consistent approach, the easy applicability of our results to observations, and our accounting for theoretical uncertainties—distinguishes our work from others in the literature.

This paper is organized as follows: we describe our model for shock evolution, particle acceleration, and magnetic field amplification in Chapter 2. In Chapter 3, we summarize the results of our $E_{\rm max}$ calculations, discussing their implications for potential PeVatron

candidates and searches in Chapter 4. We conclude in Chapter 5.

Chapter 2

Method

To calculate $E_{\max}$ for an arbitrary shock, we use a multi-zone model of particle acceleration employed in [2] and references therein. Broadly speaking we choose model parameters to be consistent with typical SNRs. However, our results can be scaled up or down to approximate the maximum energy accelerated by other types of astrophysical shocks. Note that, throughout this paper, subscripts 0, 1, and 2 are used to denote quantities far upstream, immediately upstream, and downstream of a shock.

2.1 Shock Hydrodynamics

To estimate typical SNR evolution, we employ a formalism similar to that described in [45], which assumes that ejecta and swept-up material form a thin shell behind the forward shock, which expands due to pressure from a hot bubble inside it [see, e.g., 46–48, for examples of this *thin-shell approximation*]. More specifically, we model SNRs during two stages of evolution: the *ejecta-dominated stage*, in which the mass of swept-up material is less than the ejecta mass and the shock expands freely, and the *Sedov-Taylor stage*, in which the swept-up mass exceeds the ejecta mass and the shock expands adiabatically.

Because energy conserved throughout both stages, we can write this evolution as,

$$v_{\rm sh} = \left(\frac{2E_{\rm SN}}{M_{\rm ej} + M_{\rm SU}}\right)^{1/2}, \tag{2.1}$$

where, $v_{\rm sh}$ is the forward shock velocity, $E_{\rm SN}$ is the initial SN kinetic energy, $M_{\rm ej}$ is the ejecta mass, and $M_{\rm SU}$ is the swept up mass, given by,

$$M_{\rm SU} = \int_{R_{\rm min}}^{R_{\rm sh}} 4\pi r^2 \rho_0(r) dr. \tag{2.2}$$

Eventually, the temperature behind the forward shock drops below 10^6 K and the SNR becomes radiative. However, at this point, the shock has slowed substantially such that $E_{\rm max}$ has fallen well below its peak. Put another way, the DSA timescale for CRs of energy $E = E_{\rm max}$ is given by $\tau_{\rm DSA} \approx D(E_{\rm max})/v_{\rm sh}^2$ where $D(E)$ is the energy-dependent diffusion coefficient. Assuming Bohm diffusion [49], $D(E) \propto r_{\rm L} \propto E/B_2$ where $r_{\rm L}$ is the Larmor radius and B_2 is the postshock magnetic field. This gives $E_{\rm max} \propto B_2 v_{\rm sh}^2 t$ and, since $v_{\rm sh}$ is roughly constant during the ejecta dominated stage, $E_{\rm max}$ initially increases, provided that B_2 remains constant (as is likely to be the case in a uniform ambient medium). After the transition to the Sedov stage, the shock slows down such that $v_{\rm sh} \propto t^{-3/5}$, meaning that $E_{\rm max}$ decreases with time, i.e., $E_{\rm max} \propto B_2(t) t^{-1/5}$ [1, 31]. This decrease in $E_{\rm max}$ happens even earlier for shocks expanding into a wind profile ($n \propto r^{-2}$), since the decrease in density also leads to a decrease in the amplified postshock magnetic field. Thus, $E_{\rm max}$ depends most strongly on shock evolution during the ejecta-dominated and early Sedov-Taylor stages, and we do not model the onset of the radiative stage.

Throughout this work, we consider a benchmark SNR with $E_{\rm SN} = 10^{51}$ erg and $M_{\rm ej} = 1 M_\odot$, expanding into uniform media of number density $n_{\rm ISM} \in [10^{-2}, 10^2]$ cm^{-3} (i.e., the environments around typical Type Ia SNe), and into wind profiles given by $n_{\rm ISM} \in [10^{-1}, 10] \times 3.5 (R/{\rm pc})^{-2}$ cm^{-3} (i.e., the environments around typical core-collapse SNe). Note that $n_{\rm ISM} = 3.5 (R/{\rm pc})^{-2}$ cm^{-3} corresponds to a stellar wind with velocity 10 km s^{-1}

and mass-loss rate $10^{-5} M_\odot$ yr^{-1} [e.g., 50]. To accommodate for the wide diversity of core-collapse SNe, we also consider SNRs with $E_{\rm SN} = 10^{52}$ erg and $M_{\rm ej} = 5 M_\odot$, all expanding into wind profiles.

2.2 Particle Acceleration

We model particle acceleration using a semi-analytic framework that self-consistently solves the diffusion-advection equation for the transport of non-thermal particles in a quasi-parallel, non-relativistic shock, including the dynamical effects of accelerated particles and CR-driven magnetic field amplification [see 2, 51–54, and references therein, in particular [55–60]]. We assume that protons with momenta above $p_{\rm inj} \equiv \xi_{\rm inj} p_{\rm th}$ are injected into the acceleration process, where $p_{\rm th}$ is the thermal momentum and we choose $\xi_{\rm inj}$ to produce CR pressure fractions $\sim 10\%$, consistent with kinetic simulations of quasi-parallel shocks [e.g., 61]. We also calculate $E_{\rm max}$ self-consistently by requiring that the diffusion length (assuming Bohm diffusion) of particles with energy $E = E_{\rm max}$ be 10% of the shock radius (see Section 2.4 for a detailed discussion).

This model calculates an instantaneous spectrum of protons accelerated at each timestep of shock evolution. These spectra are then shifted and weighted to account for adiabatic losses [see 7, 8, 54, for more details], before being added together to produce the cumulative, multi-zone spectrum of particles accelerated by an arbitrary shock.

It is worth noting that this model also includes the effect of the *postcursor*, a drift of CRs and magnetic fluctuations with respect to the plasma behind the shock that arises in kinetic simulations [62, 63]. This drift moves away from the shock with a velocity comparable to the local Alfvén speed in the amplified magnetic field, sufficient to produce a substantial steepening of the CR spectrum consistent with observations [see 2, for a detailed discussion]. While this effect has little bearing on the value $E_{\rm max}$, it has important consequences for the number of CRs produced at this energy. A detailed discussion of these consequences can be

found in Chapter 4.

2.3 Magnetic Field Amplification

The propagation of CRs ahead of the shock is expected to excite streaming instabilities, [14, 22, 23, 64], which drive magnetic field amplification and suppress the CR diffusion coefficient [49, 65]. The result is magnetic field perturbations with magnitudes that far exceed that of the ordered background magnetic field. This magnetic field amplification has been inferred observationally from the X-ray emission of many young SNRs, which exhibit narrow X-ray rims due to synchrotron losses by relativistic electrons [e.g., 27–29, 66]. Such magnetic field amplification is also essential for SNRs to accelerate protons to even the multi-TeV energies inferred from γ-ray observations of historical remnants [e.g., 8, 67], implying that a proper treatment of magnetic field amplification is essential to predict $E_{\rm max}$.

We model magnetic field amplification by assuming pressure contributions from both the resonant streaming instability [e.g., 14, 68–73], and the non-resonant hybrid instability [22]. Detailed discussions of these instabilities can also be found in [35].

In the resonant instability, CRs excite Alfvén waves with a wavelength equal to their gyroradius. This instability saturates when the magnitude of the resulting magnetic perturbations reaches that of the ordered background field: $\delta B/B \sim 1$. [60] derives the magnetic pressure at saturation, $P_{\rm B1,res}$, to be,

$$P_{\rm B1,res} = \frac{P_{\rm CR,1}}{4M_{\rm A,0}}, \tag{2.3}$$

where $P_{\rm CR,1}$ is the CR pressure in front of the shock and $M_{\rm A} \equiv v_{\rm sh}/v_{\rm A,0}$ is the Alfvénic Mach number.

For the fast shocks considered in this work, much more significant is the non-resonant hybrid instability. Driven by CR currents in the upstream, [22] predicts that saturation occurs when the magnetic field pressure in front of the shock, $P_{\rm B1,Bell}$, reaches approximate

equipartition with the anisotropic fraction of the CR pressure, yielding,

$$P_{\rm B1,Bell} = \frac{v_{\rm sh}}{2c}\frac{P_{\rm CR,1}}{\gamma_{\rm CR}-1}. \tag{2.4}$$

See also [74]. Here, c is the speed of light and $\gamma_{\rm CR} = 4/3$ is the CR adiabatic index. This saturation can lead to $\delta B/B_0 \gg 1$ and dominates in SNR-like environments.

That being said, a comprehensive theory for CR-driven magnetic field amplification upstream of a shock is still missing. Namely, it remains unclear whether the particles responsible for the CR currents that drive the non-resonant instability are primarily those diffusing near the shock [e.g., 22, 60] or those escaping in the far upstream [e.g., 1, 75, 76]. On the one hand, diffusing particles with energies $E < E_{\rm max}$ are greater in number. On the other, escaping particles with energy $E = E_{\rm max}$ have a larger drift speed. Thus, the relative contribution from each population should depend on the spectral slope, as discussed in [35].

In order to bracket this uncertainty, we consider two extreme scenarios:

A: Diffusing CRs are solely responsible for magnetic field amplification, such that $P_{\rm B,Bell}(x) \propto P_{\rm CR}(x)$. This scenario gives a lower limit on the amplified magnetic field and thus $E_{\rm max}$.

B: Escaping CRs are solely responsible for magnetic field amplification, such that $P_{\rm B,Bell}(x) = P_{\rm B1,Bell}$. This scenario gives an upper limit on the amplified magnetic field and thus $E_{\rm max}$.

Assuming that all components of the magnetic perturbations upstream are compressed, the downstream magnetic field strength is given by $B_2 \simeq R_{\rm sub}B_1$, where $R_{\rm sub} = u_1/u_2$ is the subshock compression ratio. Our typical SNR parameters give B_2 near a few hundred μG, in good agreement with X-ray observations of young SNRs [26, 27, 77].

Note that, throughout this work, we consider a uniform ambient magnetic field equal to that of the ISM: $B_0 = 3\mu$G. While this value may not hold in a stellar wind, changing B_0 has negligible impact on $E_{\rm max}$, since the ordered magnetic field is not responsible for confining

particles and the turbulent field amplified via the non-resonant instability does not depend on B_0.

2.4 The Maximum Energy

As mentioned in Section 2.2, the maximum energy accelerated at any given time (i.e., the instantaneous $E_{\rm max}$) is set by equating the diffusion length of protons with energy $E = E_{\rm max}$ with the size of the acceleration region, taken to be 10% the radius of the SNR, $R_{\rm sh}$, (roughly the extent of the swept-up ambient material behind the shock). Thus, we have $D(E_{\rm max})/v_{\rm sh} = 0.1R_{\rm sh}$. Assuming Bohm diffusion [e.g., 49], we obtain, $E_{\rm max} \propto B_2 v_{\rm sh} R_{\rm sh}$, which is equivalent to the age-limited scaling relation derived in Section 2.1. Combined with our prescription for magnetic field amplification in the case that non-resonant instability dominates, this scaling relation becomes,

$$E_{\rm max} \propto n_{\rm ISM}^{1/2} v_{\rm sh}^{5/2} R_{\rm sh}, \tag{2.5}$$

assuming that the CR pressure is a fixed fraction of the ram pressure, $\propto n_{\rm ISM} v_{\rm sh}^2$.

More specifically, when solving the transport equation for nonthermal particles, we require the distribution function to vanish at a distance $0.1R_{\rm sh}$ upstream of the shock, mimicking the presence of a free-escape boundary beyond which particles cannot diffuse back to the shock [see 52, for a detailed discussion]. The instantaneous escape flux is also calculated as the flux of particles crossing this boundary.

After adding together the weighted instantaneous proton spectra as described in Section 2.2, we approximate the cumulative $E_{\rm max}$ as the energy associated with the maximum of the cumulative escape flux. This energy is roughly equal to the energy at which the proton distribution drops by one e-fold [76].

Chapter 3

Results

Cumulative proton spectra from our benchmark SNR are shown in Figure 3.1 with the left (right) column corresponding to the case in which diffusing (escaping) particles drive magnetic field amplification. The top and bottom rows correspond to expansion into a typical uniform medium ($n_{\rm ISM} = 1$ cm^{-3}) and wind profile ($n_{\rm ISM} = 3.5(R/{\rm pc})^{-2}$ cm^{-3}), respectively. In these cases, $E_{\rm max}$ reaches PeV energies only under select conditions. Namely, SNRs can only be PeVatrons under the optimistic assumption that escaping particles drive magnetic field amplification and, even then, can only produce PeV particles for a brief period at roughly $t \sim 100$ yr for the uniform case and prior to $t \sim 100$ yr for the wind case. This result is broadly consistent with results in the literature [e.g., 1, 35], which find that typical SNRs are not likely to be PeVatrons.

Note that the spectra shown in Figure 3.1 are steeper than the canonical $\Phi(E) \propto E^{-2}$ predicted by standard DSA [e.g., 14]. This steepening arises from the *postcursor* effect described in Section 2.2, and is consistent with γ-ray observations of historical SNRs [e.g., 78–80].

A more detailed picture of the temporal evolution of $E_{\rm max}$ can be found in Figure 3.2, which plots $E_{\rm max}$ as a function of shock age. Bands span the range between our limiting assumptions regarding the nature of magnetic field amplification, with red (blue) correspond-

ing to expansion into the uniform (wind) profiles used in Figure 3.1. As Figure 3.2 shows, the ambient medium strongly impacts the temporal evolution of $E_{\rm max}$, both because the amplified magnetic field depends on $n_{\rm ISM}$ and, more importantly, because the density profile regulates the evolution of the shock radius and velocity.

More specifically, recalling Equation 2.5 for the instantaneous $E_{\rm max}$ along with the fact that, in a uniform medium, $R_{\rm sh} \propto t$ during the ejecta-dominated phase and $R_{\rm sh} \propto t^{2/5}$ during the Sedov-Taylor phase, we approximate,

$$E_{\rm max} \propto \begin{cases} t & t \leq t_{\rm ST} \\ t^{-3/5} & t > t_{\rm ST}. \end{cases} \tag{3.1}$$

Here, $t_{\rm ST}$ denotes the onset of the Sedov-Taylor phase. For this reason, in a uniform medium, $E_{\rm max}$ reaches a peak around $t = t_{\rm ST}$.

Alternatively, in a wind profile, $R_{\rm sh} \propto t^{2/3}$ during the Sedov-Taylor phase. Also accounting for the dependence of $E_{\rm max}$ on $n_{\rm ISM}$ (which in turn goes as $R_{\rm sh}^{-2}$), we approximate,

$$E_{\rm max} \propto \begin{cases} \text{constant} & t \leq t_{\rm ST} \\ t^{-5/6} & t > t_{\rm ST}. \end{cases} \tag{3.2}$$

In other words, in a wind profile, $E_{\rm max}$ can only increase at very early times when it is still limited by the finite age of the system. Note that this period of increasing $E_{\rm max}$ is much shorter than the evolutionary timescale of an SNR, meaning that, for the vast majority of its life, an SNR expanding into a wind profile exhibits a constant or decreasing $E_{\rm max}$. However, due to very high densities at small radii, the highest value of $E_{\rm max}$ accelerated by SNRs expanding into wind profiles tends to exceed that accelerated by SNRs expanding into uniform media.

We also compare our $E_{\rm max}$ results to the calculation presented in [1], which sets $E_{\rm max}$ by requiring that the current of escaping particles of energy $E = E_{\rm max}$ be sufficient to

produce strong magnetic field amplification via the non-resonant streaming instability. This approximation gives an instantaneous maximum energy that scales similarly to the relations described in the preceding paragraphs (see their Equation 6), and is displayed as solid lines in Figure 3.2.

Note that while our results are in good agreement with those of [1] at early times, they diverge after $t \sim t_{\rm ST}$. This divergence also occurs when comparing our results to the scaling relations shown in Equations 3.1 and 3.2, and arises from the fact that both [1] and Equations 3.1 and 3.2 consider only a single population of particles. However, in our multi-zone framework, we account for the presence of old populations of particles with an $E_{\rm max}$ that may differ from the maximum energy currently being accelerated by the shock. As Equations 3.1 and 3.2 show, for $t > t_{\rm ST}$, these old populations have a larger $E_{\rm max}$ than the current instantaneous one, leading to a slowed decline of the cumulative maximum energy. In other words, by considering the overall evolution of the shock, we find that older shocks may produce γ-ray signatures that point toward higher $E_{\rm max}$ than would be predicted from a single-zone model.

Finally, we present $E_{\rm max}$ as a function of a more readily observable parameter, $v_{\rm sh}$, in Figure 3.3, for a variety of modeled SNRs. As in Figure 3.1, the left (right) column corresponds to the case in which diffusing (escaping) particles drive magnetic field amplification, and the top (bottom) row corresponds to expansion in to a uniform (wind) profile. However, we also consider a wider range of shock parameters, as introduced in Section 2.1: $n_{\rm ISM} \in [10^{-2}, 10^{2}]$ cm^{-3} in the uniform case and $n_{\rm ISM} \in [10^{-1}, 10] \times 3.5 (R/{\rm pc})^{-2}$ cm^{-3} in the wind case. We also consider SNRs with $E_{\rm SN} = 10^{52}$ erg and/or $M_{\rm ej} = 5 M_{\odot}$ (wind case only).

As expected from Equations 3.1 and 3.2, faster shocks have higher $E_{\rm max}$, as do shocks expanding into denser media, though this density dependence is mild (note that the normalization of $n_{\rm ISM}$ is given by the color scale in Figure 3.3). Thus, for shocks that have reached the Sedov-Taylor stage, $v_{\rm sh}$—which is more easily inferred from observations than age—serves as a good proxy for $E_{\rm max}$. However, this relationship breaks down for young,

ejecta-dominated SNRs, which have roughly constant $v_{\rm sh}$ and thus an $E_{\rm max}$ that is set by $R_{\rm sh}$. This is especially true in the uniform case, in which $E_{\rm max}$ rises prior to $t_{\rm ST}$. To emphasize this issue, points in Figure 3.3 corresponding to $t < t_{\rm ST}$ are outlined in black.

Thus, the results shown in Figure 3.3 are best summarized with an empirical relationship that includes $v_{\rm sh}$, $R_{\rm sh}$, and, to a lesser extent, $n_{\rm ISM}$. We approximate this relationship as,

$$E_{\rm max} \simeq \alpha \left(\frac{n_{\rm ISM}}{\rm cm^{-3}}\right)^{\frac{1}{2}} \left(\frac{v_{\rm sh}}{10^3 \text{ km s}^{-1}}\right)^2 \left(\frac{R_{\rm sh}}{\rm pc}\right) \text{ GeV} \tag{3.3}$$

where $\alpha = 7 \times 10^2$ if diffusing particles drive magnetic field amplification and $\alpha = 1.5 \times 10^4$ if escaping particles drive magnetic field amplification. Note that this expression retains the same scalings with $R_{\rm sh}$ and $n_{\rm ISM}$ as Equation 2.5, but has a slightly weaker dependence on $v_{\rm sh}$ ($E_{\rm max} \propto v_{\rm sh}^2$ instead of $v_{\rm sh}^{5/2}$). This weakened velocity dependence approximates the multi-zone effects described previously, namely, that old populations of particles can contribute to the cumulative $E_{\rm max}$.

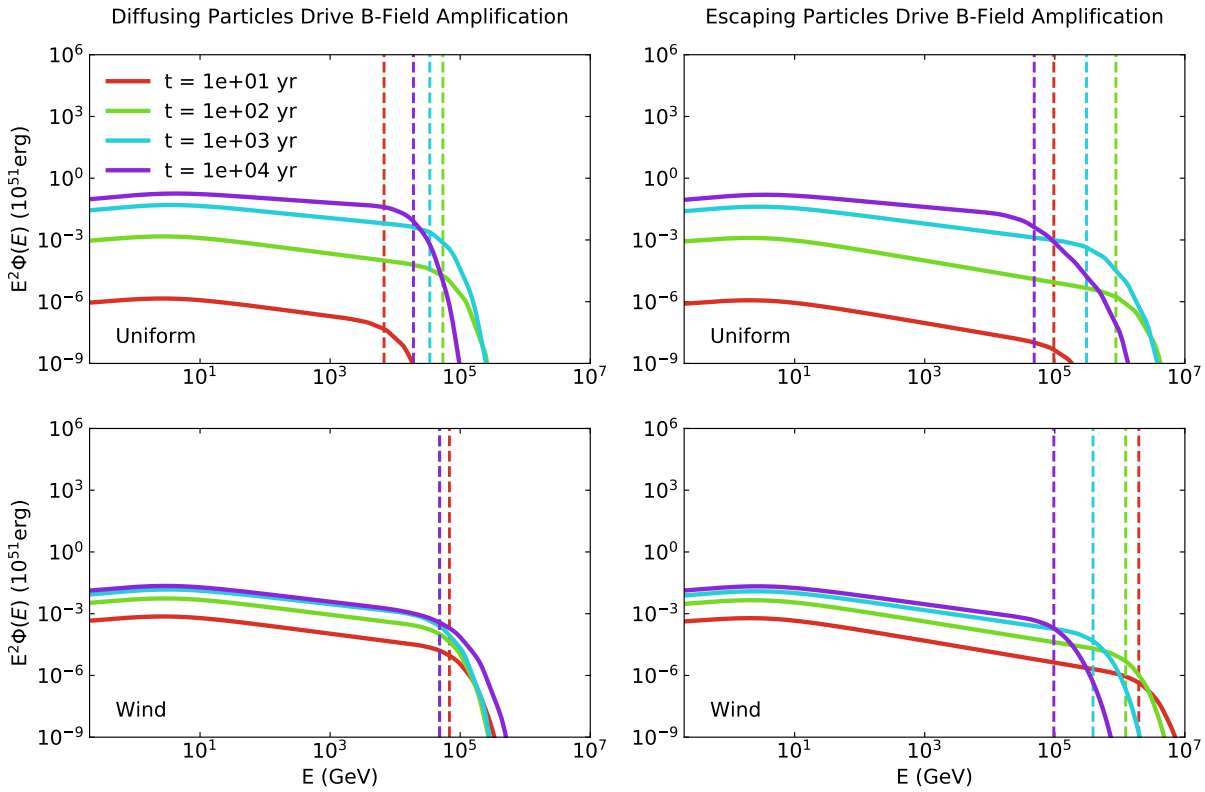

Figure 3.1: Cumulative spectra of accelerated protons produced by our benchmark SNR ($E_{\rm SN} = 10^{51}$ erg, $M_{\rm ej} = 1 M_\odot$) at different stages (denoted by line color) of shock evolution, assuming diffusing particles drive magnetic field amplification (left column) or escaping particles drive magnetic field amplification (right column). The top row of spectra corresponds to a uniform ambient medium of density of 1 cm^{-3}, while the bottom row corresponds to a wind profile of density $3.5(R/\text{pc})^{-2}$ cm^{-3}. The maximum proton energy of each spectrum is denoted with a dashed vertical line. Typical SNRs can only accelerate PeV particles if escaping CRs drive magnetic field amplification, and even then only at relatively early times ($t \sim 100$ yr).

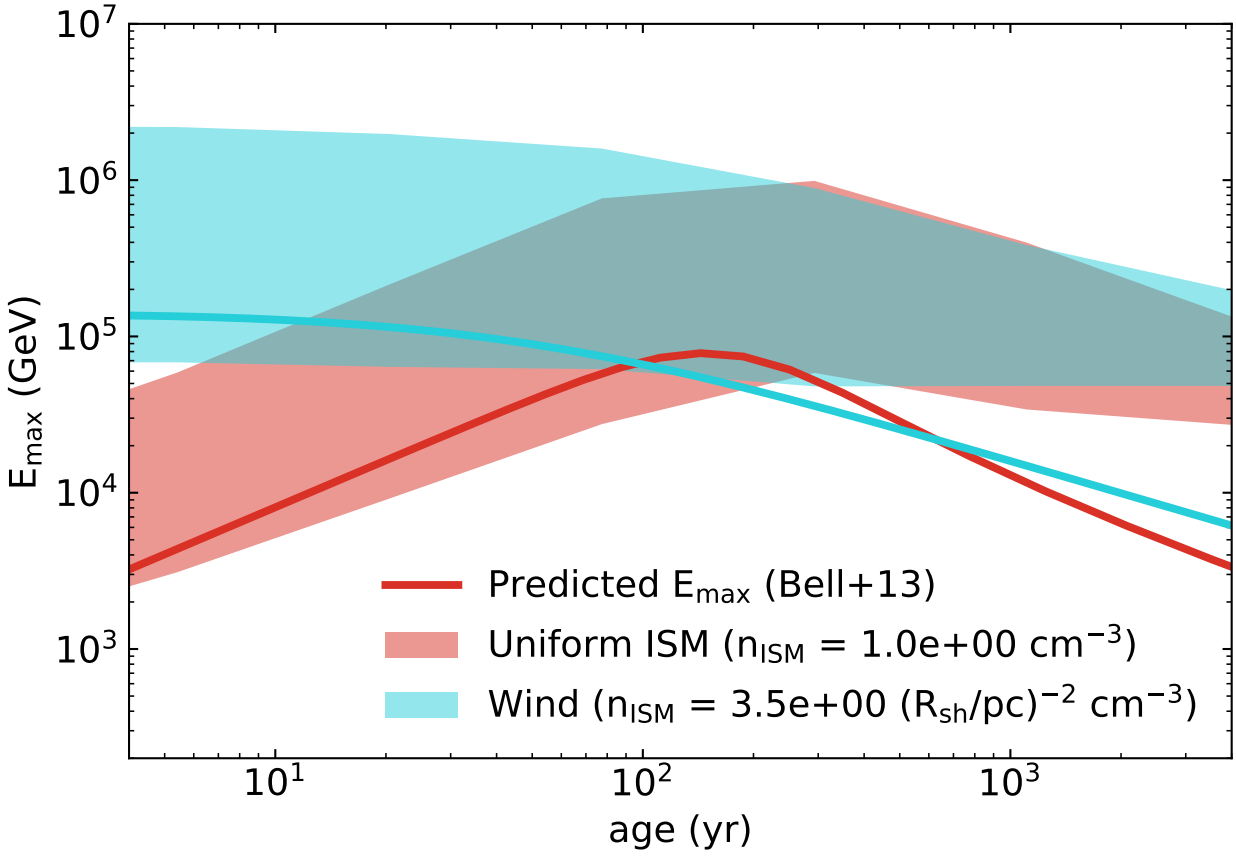

Figure 3.2: The maximum energy, $E_{\rm max}$, accelerated by our benchmark SNR as a function of time, expanding into a uniform medium (red band) and wind profile (blue band), as in Figure 3.1. The widths of the bands correspond to uncertainties in the nature of CR-driven magnetic field amplification (i.e., the lower (upper) limit assumes diffusing (escaping) particles drive amplification). Solid lines give the single-zone $E_{\rm max}$ prediction put forth in [1]. While this prediction yields good agreement with our results at early times, we predict a higher $E_{\rm max}$ at late times due to the presence of old populations of particles accelerated when the SNR was expanding more rapidly.

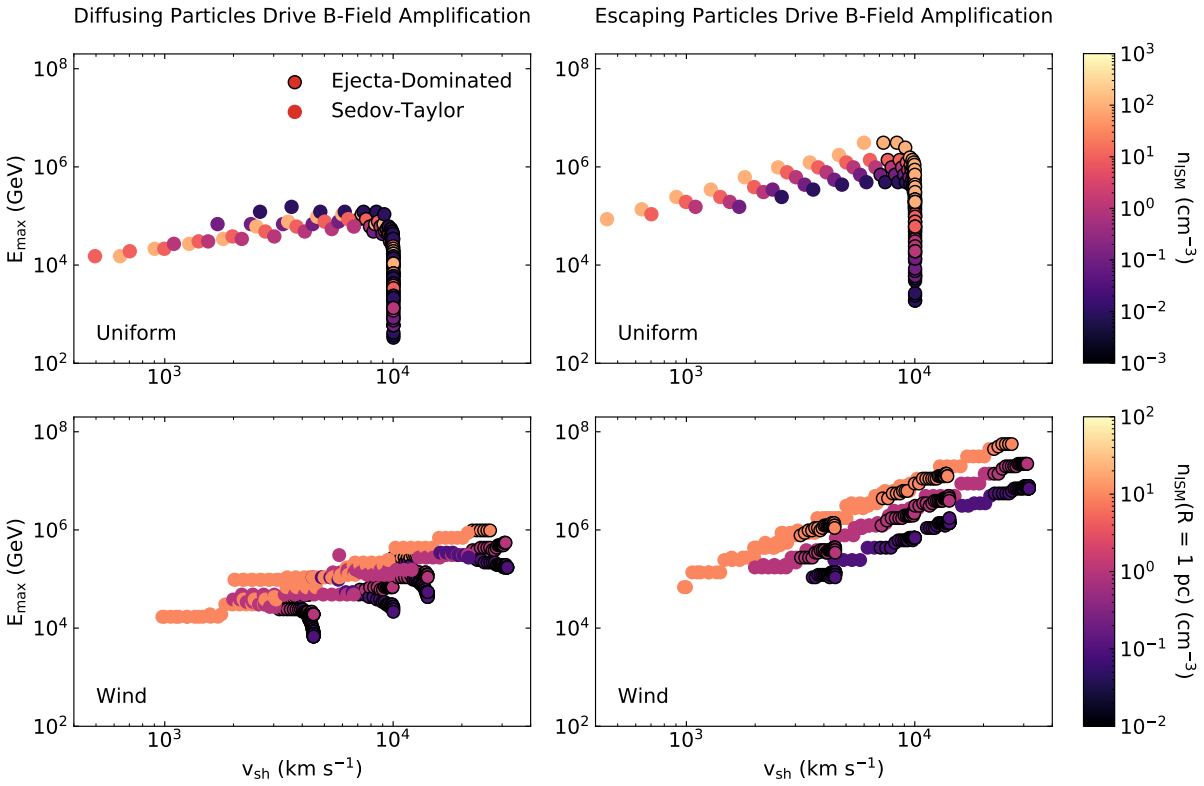

Figure 3.3: $E_{\rm max}$ as a function of shock velocity, ($v_{\rm sh}$), for a variety of SNRs expanding into media of different ambient density normalizations (color scales), assuming diffusing particles drive magnetic field amplification (left column) or escaping particles drive magnetic field amplification (right column). The top row corresponds to expansion into uniform ambient media and, to be broadly consistent with an SNR from a Type Ia SN, only considers our benchmark scenario. Meanwhile, to capture the wider range of parameters associated with core-collapse SNe, the bottom row corresponds to expansion of SNRs into wind profiles with $E_{\rm SN} \in [1, 10] \times 10^{51}$ erg and $M_{\rm ej} \in [1, 5]\ M_{\odot}$. Outlined points denote SNRs that are still ejecta-dominated. For SNRs expanding into wind profiles, evolutionary stage has little bearing on $E_{\rm max}$ such that $v_{\rm sh}$ serves as a good predictor of its value (modulo density normalization). On the other hand, for SNRs expanding into uniform media, $v_{\rm sh}$ is only a good predictor of $E_{\rm max}$ during the Sedov-Taylor phase.

Chapter 4

Discussion

We will now discuss our results in the context of particle acceleration up to PeV energies, i.e., the approximate energy of the CR "knee."

4.1 SNRs as PeVatrons

As demonstrated in the preceding chapter, SNRs can only accelerate PeV particles under select circumstances:

1. Escaping particles must drive magnetic field amplification.
2. The shock must be expanding relatively quickly ($v_{\rm sh} \gtrsim 10^4$ km s^{-1} for $n_{\rm ISM} = 1$ cm^{-3}).
3. In the absence of a fast shock ($v_{\rm sh} \gtrsim 10^4$ km s^{-1}), the ambient number density must be $\gg 1$ cm^{-3}.

These conditions are comparable to those presented in the literature [e.g., 1, 31, 32, 34, 35, 81], which also find that only a small subset of fast SNRs expanding into dense media can be PeVatrons. Such stringent requirements may explain the dearth of observed PeVatrons that can be definitively associated with SNRs [e.g., 37]. However, in contrast to recent works in

the literature that completely rule out SNRs as PeVatrons [e.g., 36] we find that it is possible for SNRs to at least contribute to—though perhaps not saturate—the CR knee.

That being said, the fact remains that typical historical SNRs are likely incapable of accelerating PeV particles, meaning that other astrophysical accelerators may contribute to the CR spectrum at the knee. For example, [42] puts forward massive star clusters as Galactic PeVatrons. In this picture, shocks are still likely responsible for particle acceleration, meaning that the formalism and scaling relations presented in this work may be applicable.

4.2 Considerations for PeVatron Searches

A notable result from our work is the fact that SNRs and other astrophysical shocks may exhibit γ-ray and neutrino signatures of PeV particles after they are no longer accelerating them. In this case, one might expect to see ~ 100 TeV γ-rays from SNRs approaching $t \simeq 100$ yr. Of course, the question remains whether such PeV particles would remain confined and, if not, how far they would propagate away from their accelerator.

After acceleration, a particle will remain confined within an SNR provided that, downstream of the shock, diffusion is insufficient to overcome advection [see, e.g., 82]. In other words, we require that the advection timescale, $\tau_{\rm adv} \simeq R_{\rm sh}/u_2$ (where $u_2 \simeq v_{\rm sh}/4$ is the velocity of the downstream plasma in the frame of the shock), be less than the diffusion timescale, $\tau_{\rm diff} \simeq R_{\rm sh}^2/D(E)$, i.e., we require $D(E) < u_2 R_{\rm sh}$. This requirement holds for all particles except those very close to $E = E_{\rm max}$, since $D(E_{\rm max}) \sim R_{\rm sh} v_{\rm sh}$. For shocks expanding into uniform media, $R_{\rm sh} v_{\rm sh} \propto t^{-1/5}$ after $t_{\rm ST}$, meaning that confined particles will eventually escape, but only after the shock has evolved for a long time. For shocks expanding into wind profiles, $R_{\rm sh} v_{\rm sh} \propto t^{1/3}$ after $t_{\rm ST}$, meaning that initially-confined particles are likely to remain so. In short, a shock that accelerates PeV particles may be able to confine them even after it is no longer capable of accelerating them.

Of course, $D(E)$ may also grow with time if, for example, magnetic turbulence is damped.

However, even in the case that PeV particles quickly escape their accelerators, they may produce detectable γ-ray signatures in the vicinity. Namely, taking the canonical diffusion coefficient in our Galaxy, $D(E) \simeq 3 \times 10^{28} (E/\mathrm{GeV})^{1/3}$ cm^2 s [i.e., the maximum possible value of $D(E)$, see, e.g., 83], PeV particles will only diffuse ~ 100 pc after ~ 1000 yr. Moreover, in a uniform medium, the γ-ray and neutrino luminosities due to proton-proton collisions between these PeV particles and the ISM will remain constant as the CRs diffuse away, albeit smaller than it would have been had particles remained confined to the denser medium downstream of the shock. The exact luminosity will depend on the fraction of particles that escape, along with the nature of the nearby medium [e.g., the presence of molecular clouds, 84]. This consideration is especially important for water-Cherenkov observatories such as LHASSO and HAWC (and potentially the next generation of neutrino detectors, e.g., KM3NET, IceCube–Gen2, TRIDENT, P-One), which have comparatively lower resolutions than atmospheric Cherenkov telescopes and thus higher sensitivities to extended sources.

Finally, it is worth noting that the *postcursor* effect, introduced in Section 2.2, has implications for PeVatron searches with γ-ray observatories or neutrino detectors, particularly those that select sources based on their γ-ray luminosities at lower energies [e.g., 85]. Namely, in this paradigm, faster shocks, which exhibit stronger amplified magnetic fields via the non-resonant instability, are expected to have faster-drifting magnetic fluctuations and thus steeper spectra. This expectation is also consistent with observations of both historical SNRs and young, extragalactic SNe [2].

Thus, if fast shocks tend to accelerate CRs with steeper spectra, the ostensible best candidates to be PeVatrons will have small CR luminosities at PeV energies (L_{PeV}) relative to their CR luminosities at, say, GeV energies (L_{GeV}). And, since hadronic γ-ray and neutrino emissions have the same spectral slope as that of the parent protons, this effect will be reproduced in observations. We summarize this effect in Figure 4.1, which shows $L_{\mathrm{PeV}}/L_{\mathrm{GeV}}$ as a function of v_{sh} for all modeled SNRs with $E_{\mathrm{max}} > 1$ PeV. Note that, regardless of the

slope of the underlying particle population(s), γ-ray emission at TeV energies is likely to be hadronic in origin, since the maximum energy of leptons is limited by synchrotron losses [86].

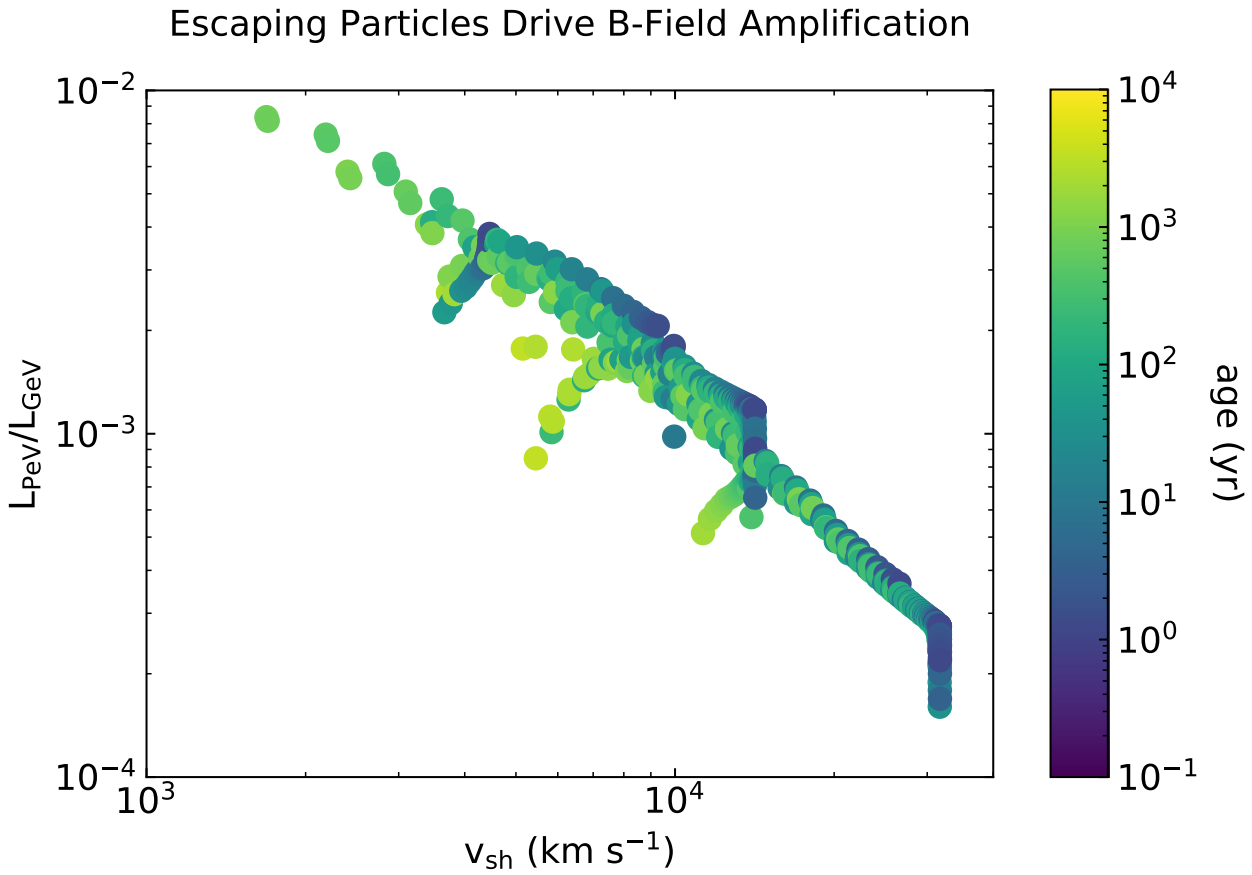

Figure 4.1: PeV to GeV proton luminosity ratio ($L_{\rm PeV}/L_{\rm GeV}$) as a function of $v_{\rm sh}$ for SNR PeVatron candidates (i.e., data points from Figure 3.3 with $E_{\rm max} > 10^6$ GeV). Shock age is denoted with the color scale. Due to the *postcursor* effect [2, see text for details], faster shocks—which are the best candidates to accelerate PeV particles—likely produce steeper spectra, and thus exhibit lower $L_{\rm PeV}/L_{\rm GeV}$. This effect is important for PeVatron searches that select observational targets based on their γ-ray luminosities at lower energies.

Chapter 5

Conclusion

In summary, we placed constraints on the maximum proton energy, $E_{\rm max}$, accelerated by an arbitrary astrophysical shock using a self-consistent, multi-zone model of particle acceleration, including the dynamical back-reaction of CRs on the shock as well as a prescription for magnetic field amplification that brackets theoretical uncertainties. We presented our results in terms of parameters that can be constrained observationally, in particular the shock velocity (see Equation 3.3). We also analyzed our results in the context of CR acceleration to PeV energies and discussed considerations for observational PeVatron searches.

Consistent with results presented in the literature, we find that typical historical SNRs cannot accelerate particles to PeV energies. However, young, fast SNRs expanding into dense media can be PeVatrons if escaping particles drive magnetic field amplification.

We also find that old populations of particles can contribute to the cumulative spectrum accelerated by an astrophysical shock. This implies that SNRs and other cosmic accelerators may exhibit a higher $E_{\rm max}$ than they are currently capable of accelerating or, equivalently, that former PeVatrons may still produce $\gtrsim 100$ TeV γ-ray emission.

Finally, we note that, due to the drift of magnetic fluctuations with the local Alfvén speed downstream of astrophysical shocks (the *postcursor*), fast shocks—which are the best candidates to produce PeV particles—have steeper spectra than their slower counterparts. In other

words, compared to a slower counterpart, a fast shock will have a smaller PeV luminosity relative to its luminosity at lower energies. This consideration is important for observational PeVatron searches that select targets based on their GeV or TeV γ-ray luminosities.

These results serve as a reference to modelers seeking to estimate $E_{\rm max}$ for an arbitrary astrophysical shock, particularly in anticipation of the next generation of γ-ray and neutrino telescopes (e.g., The Cherenkov Telescope Array, IceCube–Gen2), which will better constrain the source(s) of PeV CRs in the coming years [see, e.g., 85, 87].

References

[1] A. R. Bell, K. M. Schure, B. Reville, and G. Giacinti. Cosmic-ray acceleration and escape from supernova remnants. *MNRAS*, 431:415–429, May 2013.

[2] Rebecca Diesing and Damiano Caprioli. Steep Cosmic-Ray Spectra with Revised Diffusive Shock Acceleration. , 922(1):1, November 2021.

[3] Rebecca Diesing. The Maximum Energy of Shock-Accelerated Cosmic Rays. *arXiv e-prints*, page arXiv:2305.07697, May 2023.

[4] A. M. Hillas. TOPICAL REVIEW: Can diffusive shock acceleration in supernova remnants account for high-energy galactic cosmic rays? *Journal of Physics G Nuclear Physics*, 31:95–+, May 2005.

[5] E. G. Berezhko and H. J. Völk. Spectrum of Cosmic Rays Produced in Supernova Remnants. , 661:L175–L178, June 2007.

[6] V. Ptuskin, V. Zirakashvili, and E.-S. Seo. Spectrum of Galactic Cosmic Rays Accelerated in Supernova Remnants. , 718:31–36, July 2010.

[7] D. Caprioli, E. Amato, and P. Blasi. The contribution of supernova remnants to the galactic cosmic ray spectrum. *APh*, 33:160–168, April 2010.

[8] G. Morlino and D. Caprioli. Strong evidence for hadron acceleration in Tycho's supernova remnant. *A&A*, 538:A81, February 2012.

[9] P. Slane, S.-H. Lee, D. C. Ellison, D. J. Patnaude, J. P. Hughes, K. A. Eriksen, D. Castro, and S. Nagataki. A cr-hydro-nei model of the structure and broadband emission from tycho's supernova remnant. , 783:33, March 2014.

[10] M. Ackermann et al. Detection of the Characteristic Pion-Decay Signature in Supernova Remnants. *Science*, 339:807–811, February 2013.

[11] E. Fermi. Galactic Magnetic Fields and the Origin of Cosmic Radiation. *Ap. J.*, 119:1–+, January 1954.

[12] G. F. Krymskii. A regular mechanism for the acceleration of charged particles on the front of a shock wave. *Akademiia Nauk SSSR Doklady*, 234:1306–1308, June 1977.

[13] W. I. Axford, E. Leer, and G. Skadron. Acceleration of Cosmic Rays at Shock Fronts (Abstract). In Acceleration of Cosmic Rays at Shock Fronts, volume 2 of *International Cosmic Ray Conference*, pages 273–+, 1977.

[14] A. R. Bell. The acceleration of cosmic rays in shock fronts. I. *MNRAS*, 182:147–156, January 1978.

[15] R. D. Blandford and J. P. Ostriker. Particle acceleration by astrophysical shocks. *ApJL*, 221:L29–L32, April 1978.

[16] M. Ajello, D. Caprioli, Diesing, , and Fermi-LAT Collaboration. Gamma Rays from Fast Black-hole Winds. , 921(2):144, November 2021.

[17] Rebecca Diesing, Brian D. Metzger, Elias Aydi, Laura Chomiuk, Indrek Vurm, Siddhartha Gupta, and Damiano Caprioli. Evidence for multiple shocks from the -ray emission of rs ophiuchi. *The Astrophysical Journal*, 947(2):70, apr 2023.

[18] Johannes Blümer, Ralph Engel, and Jörg R. Hörandel. Cosmic rays from the knee to the highest energies. *Progress in Particle and Nuclear Physics*, 63(2):293–338, 2009.

[19] B. Bartoli, P. Bernardini, X. J. Bi, Z. Cao, S. Catalanotti, S. Z. Chen, T. L. Chen, S. W. Cui, B. Z Dai, A. D'Amone, Danzengluobu, I. De Mitri, B. D'Ettorre Piazzoli, T. Di Girolamo, G. Di Sciascio, C. F. Feng, Zhaoyang Feng, Zhenyong Feng, Q. B. Guo, Y. Q. Guo, H. H. He, Haibing Hu, Hongbo Hu, M. Iacovacci, R. Iuppa, H. Y. Jia, Labaciren, H. J. Li, C. Liu, J. Liu, M. Y. Liu, H. Lu, L. L. Ma, X. H. Ma, G. Mancarella, S. M. Mari, G. Marsella, S. Mastroianni, P. Montini, C. C. Ning, L. Perrone, P. Pistilli, P. Salvini, R. Santonico, P. R. Shen, X. D. Sheng, F. Shi, A. Surdo, Y. H. Tan, P. Vallania, S. Vernetto, C. Vigorito, H. Wang, C. Y. Wu, H. R. Wu, L. Xue, Q. Y. Yang, X. C. Yang, Z. G. Yao, A. F. Yuan, M. Zha, H. M. Zhang, L. Zhang, X. Y. Zhang, Y. Zhang, J. Zhao, Zhaxiciren, Zhaxisangzhu, X. X. Zhou, F. R. Zhu, Q. Q. Zhu, Y. X. Bai, M. J. Chen, S. H. Feng, B. Gao, M. H. Gu, C. Hou, J. Liu, J. L. Liu, X. Wang, G. Xiao, B. K. Zhang, S. S. Zhang, B. Zhou, and X. Zuo. Knee of the cosmic hydrogen and helium spectrum below 1 pev measured by argo-ybj and a cherenkov telescope of lhaaso. *Phys. Rev. D*, 92:092005, Nov 2015.

[20] IceCube Collaboration, R. Abbasi, Y. Abdou, M. Ackermann, J. Adams, J. A. Aguilar, M. Ahlers, D. Altmann, K. Andeen, J. Auffenberg, X. Bai, M. Baker, S. W. Barwick, V. Baum, R. Bay, K. Beattie, J. J. Beatty, S. Bechet, J. K. Becker, K. H. Becker, M. Bell, M. L. Benabderrahmane, S. BenZvi, J. Berdermann, P. Berghaus, D. Berley, E. Bernardini, D. Bertrand, D. Z. Besson, D. Bindig, M. Bissok, E. Blaufuss, J. Blumenthal, D. J. Boersma, C. Bohm, D. Bose, S. Böser, O. Botner, L. Brayeur, A. M. Brown, R. Bruijn, J. Brunner, S. Buitink, K. S. Caballero-Mora, M. Carson, J. Casey, M. Casier, D. Chirkin, B. Christy, F. Clevermann, S. Cohen, D. F. Cowen, A. H. Cruz Silva, M. Danninger, J. Daughhetee, J. C. Davis, C. De Clercq, F. Descamps, P. Desiati, G. de Vries-Uiterweerd, T. DeYoung, J. C. Díaz-Vélez, J. Dreyer, J. P. Dumm, M. Dunkman, R. Eagan, J. Eisch, R. W. Ellsworth, O. Engdegård, S. Euler, P. A. Evenson, O. Fadiran, A. R. Fazely, A. Fedynitch, J. Feintzeig, T. Feusels, K. Filimonov, C. Finley, T. Fischer-Wasels, S. Flis, A. Franckowiak, R. Franke, K. Frantzen, T. Fuchs, T. K.

Gaisser, J. Gallagher, L. Gerhardt, L. Gladstone, T. Glüsenkamp, A. Goldschmidt, J. A. Goodman, D. Góra, D. Grant, A. Groß, S. Grullon, M. Gurtner, C. Ha, A. Haj Ismail, A. Hallgren, F. Halzen, K. Hanson, D. Heereman, P. Heimann, D. Heinen, K. Helbing, R. Hellauer, S. Hickford, G. C. Hill, K. D. Hoffman, R. Hoffmann, A. Homeier, K. Hoshina, W. Huelsnitz, P. O. Hulth, K. Hultqvist, S. Hussain, A. Ishihara, E. Jacobi, J. Jacobsen, G. S. Japaridze, O. Jlelati, H. Johansson, A. Kappes, T. Karg, A. Karle, J. Kiryluk, F. Kislat, J. Kläs, S. R. Klein, J. H. Köhne, G. Kohnen, H. Kolanoski, L. Köpke, C. Kopper, S. Kopper, D. J. Koskinen, M. Kowalski, M. Krasberg, G. Kroll, J. Kunnen, N. Kurahashi, T. Kuwabara, M. Labare, K. Laihem, H. Landsman, M. J. Larson, R. Lauer, M. Lesiak-Bzdak, J. Lünemann, J. Madsen, R. Maruyama, K. Mase, H. S. Matis, F. McNally, K. Meagher, M. Merck, P. Mészáros, T. Meures, S. Miarecki, E. Middell, N. Milke, J. Miller, L. Mohrmann, T. Montaruli, R. Morse, S. M. Movit, R. Nahnhauer, U. Naumann, S. C. Nowicki, D. R. Nygren, A. Obertacke, S. Odrowski, A. Olivas, M. Olivo, A. O'Murchadha, S. Panknin, L. Paul, J. A. Pepper, C. Pérez de los Heros, D. Pieloth, N. Pirk, J. Posselt, P. B. Price, G. T. Przybylski, L. Rädel, K. Rawlins, P. Redl, E. Resconi, W. Rhode, M. Ribordy, M. Richman, B. Riedel, J. P. Rodrigues, F. Rothmaier, C. Rott, T. Ruhe, D. Rutledge, B. Ruzybayev, D. Ryckbosch, T. Salameh, H. G. Sander, M. Santander, S. Sarkar, S. M. Saba, K. Schatto, M. Scheel, F. Scheriau, T. Schmidt, M. Schmitz, S. Schoenen, S. Schöneberg, L. Schönherr, A. Schönwald, A. Schukraft, L. Schulte, O. Schulz, D. Seckel, S. H. Seo, Y. Sestayo, S. Seunarine, M. W. E. Smith, M. Soiron, D. Soldin, G. M. Spiczak, C. Spiering, M. Stamatikos, T. Stanev, A. Stasik, T. Stezelberger, R. G. Stokstad, A. Stößl, E. A. Strahler, R. Ström, G. W. Sullivan, H. Taavola, I. Taboada, A. Tamburro, S. Ter-Antonyan, S. Tilav, P. A. Toale, S. Toscano, M. Usner, N. van Eijndhoven, D. van der Drift, A. Van Overloop, J. van Santen, M. Vehring, M. Voge, C. Walck, T. Waldenmaier, M. Wallraff, M. Walter, R. Wasserman, Ch. Weaver, C. Wendt, S. Westerhoff, N. Whitehorn, K. Wiebe, C. H. Wiebusch, D. R. Williams, H. Wissing, M. Wolf, T. R.

Wood, K. Woschnagg, C. Xu, D. L. Xu, X. W. Xu, J. P. Yanez, G. Yodh, S. Yoshida, P. Zarzhitsky, J. Ziemann, A. Zilles, and M. Zoll. Cosmic ray composition and energy spectrum from 1-30 PeV using the 40-string configuration of IceTop and IceCube. *Astroparticle Physics*, 42:15–32, February 2013.

[21] P. O. Lagage and C. J. Cesarsky. The maximum energy of cosmic rays accelerated by supernova shocks. , 125:249–257, September 1983b.

[22] A. R. Bell. Turbulent amplification of magnetic field and diffusive shock acceleration of cosmic rays. *MNRAS*, 353:550–558, September 2004.

[23] E. Amato and P. Blasi. A kinetic approach to cosmic-ray-induced streaming instability at supernova shocks. *MNRAS*, 392:1591–1600, February 2009.

[24] B. Reville and A. R. Bell. A filamentation instability for streaming cosmic rays. *MNRAS*, 419:2433–2440, January 2012.

[25] Georgios Zacharegkas, Damiano Caprioli, and Colby Haggerty. Modeling the Saturation of the Bell Instability using Hybrid Simulations. *arXiv e-prints*, page arXiv:2210.08072, October 2022.

[26] H. J. Völk, E. G. Berezhko, and L. T. Ksenofontov. Magnetic field amplification in Tycho and other shell-type supernova remnants. *A&A*, 433:229–240, April 2005.

[27] E. Parizot et al. Observational constraints on energetic particle diffusion in young supernovae remnants: amplified magnetic field and maximum energy. *A&A*, 453:387–395, July 2006.

[28] G. Morlino, E. Amato, P. Blasi, and D. Caprioli. Spatial structure of X-ray filaments in SN 1006. , 405:L21–L25, June 2010.

[29] S. M. Ressler et al. Magnetic Field Amplification in the Thin X-Ray Rims of SN1006. , 790:85, August 2014.

[30] A. Tran, B. J. Williams, R. Petre, S. M. Ressler, and S. P. Reynolds. Energy dependence of synchrotron x-ray rims in tycho's supernova remnant. , 812:101, October 2015.

[31] Martina Cardillo, Elena Amato, and Pasquale Blasi. On the cosmic ray spectrum from type ii supernovae expanding in their red giant presupernova wind. *Astroparticle Physics*, 69:1–10, 2015.

[32] Alexandre Marcowith, Vikram V. Dwarkadas, Matthieu Renaud, Vincent Tatischeff, and Gwenael Giacinti. Core-collapse supernovae as cosmic ray sources. , 479(4):4470–4485, October 2018.

[33] Stefano Gabici, Carmelo Evoli, Daniele Gaggero, Paolo Lipari, Philipp Mertsch, Elena Orlando, Andrew Strong, and Andrea Vittino. The origin of Galactic cosmic rays: Challenges to the standard paradigm. *International Journal of Modern Physics D*, 28(15):1930022–339, January 2019.

[34] Pierre Cristofari, Pasquale Blasi, and Elena Amato. The low rate of galactic pevatrons. *Astroparticle Physics*, 123:102492, 2020.

[35] P. Cristofari, P. Blasi, and D. Caprioli. Cosmic ray protons and electrons from supernova remnants. , 650:A62, June 2021.

[36] R Brose, I Sushch, and J Mackey. Core-collapse supernovae in dense environments – particle acceleration and non-thermal emission. *Monthly Notices of the Royal Astronomical Society*, 516(1):492–505, 08 2022.

[37] Zhen Cao, F. A. Aharonian, Q. An, L. X. Axikegu, Bai, Y. X. Bai, Y. W. Bao, D. Bastieri, X. J. Bi, Y. J. Bi, H. Cai, J. T. Cai, Zhe Cao, J. Chang, J. F. Chang, X. C. Chang, B. M. Chen, J. Chen, L. Chen, Liang Chen, Long Chen, M. J. Chen, M. L. Chen, Q. H. Chen, S. H. Chen, S. Z. Chen, T. L. Chen, X. L. Chen, Y. Chen, N. Cheng, Y. D. Cheng, S. W. Cui, X. H. Cui, Y. D. Cui, B. Z. Dai, H. L. Dai, Z. G.

Dai, Danzengluobu, D. della Volpe, B. D'Ettorre Piazzoli, X. J. Dong, J. H. Fan, Y. Z. Fan, Z. X. Fan, J. Fang, K. Fang, C. F. Feng, L. Feng, S. H. Feng, Y. L. Feng, B. Gao, C. D. Gao, Q. Gao, W. Gao, M. M. Ge, L. S. Geng, G. H. Gong, Q. B. Gou, M. H. Gu, J. G. Guo, X. L. Guo, Y. Q. Guo, Y. Y. Guo, Y. A. Han, H. H. He, H. N. He, J. C. He, S. L. He, X. B. He, Y. He, M. Heller, Y. K. Hor, C. Hou, X. Hou, H. B. Hu, S. Hu, S. C. Hu, X. J. Hu, D. H. Huang, Q. L. Huang, W. H. Huang, X. T. Huang, Z. C. Huang, F. Ji, X. L. Ji, H. Y. Jia, K. Jiang, Z. J. Jiang, C. Jin, D. Kuleshov, K. Levochkin, B. B. Li, Cong Li, Cheng Li, F. Li, H. B. Li, H. C. Li, H. Y. Li, J. Li, K. Li, W. L. Li, X. Li, Xin Li, X. R. Li, Y. Li, Y. Z. Li, Zhe Li, Zhuo Li, E. W. Liang, Y. F. Liang, S. J. Lin, B. Liu, C. Liu, D. Liu, H. Liu, H. D. Liu, J. Liu, J. L. Liu, J. S. Liu, J. Y. Liu, M. Y. Liu, R. Y. Liu, S. M. Liu, W. Liu, Y. N. Liu, Z. X. Liu, W. J. Long, R. Lu, H. K. Lv, B. Q. Ma, L. L. Ma, X. H. Ma, J. R. Mao, A. Masood, W. Mitthumsiri, T. Montaruli, Y. C. Nan, B. Y. Pang, P. Pattarakijwanich, Z. Y. Pei, M. Y. Qi, D. Ruffolo, V. Rulev, A. Sáiz, L. Shao, O. Shchegolev, X. D. Sheng, J. R. Shi, H. C. Song, Yu. V. Stenkin, V. Stepanov, Q. N. Sun, X. N. Sun, Z. B. Sun, P. H. T. Tam, Z. B. Tang, W. W. Tian, B. D. Wang, C. Wang, H. Wang, H. G. Wang, J. C. Wang, J. S. Wang, L. P. Wang, L. Y. Wang, R. N. Wang, W. Wang, W. Wang, X. G. Wang, X. J. Wang, X. Y. Wang, Y. D. Wang, Y. J. Wang, Y. P. Wang, Zheng Wang, Zhen Wang, Z. H. Wang, Z. X. Wang, D. M. Wei, J. J. Wei, Y. J. Wei, T. Wen, C. Y. Wu, H. R. Wu, S. Wu, W. X. Wu, X. F. Wu, S. Q. Xi, J. Xia, J. J. Xia, G. M. Xiang, G. Xiao, H. B. Xiao, G. G. Xin, Y. L. Xin, Y. Xing, D. L. Xu, R. X. Xu, L. Xue, D. H. Yan, C. W. Yang, F. F. Yang, J. Y. Yang, L. L. Yang, M. J. Yang, R. Z. Yang, S. B. Yang, Y. H. Yao, Z. G. Yao, Y. M. Ye, L. Q. Yin, N. Yin, X. H. You, Z. Y. You, Y. H. Yu, Q. Yuan, H. D. Zeng, T. X. Zeng, W. Zeng, Z. K. Zeng, M. Zha, X. X. Zhai, B. B. Zhang, H. M. Zhang, H. Y. Zhang, J. L. Zhang, J. W. Zhang, L. Zhang, Li Zhang, L. X. Zhang, P. F. Zhang, P. P. Zhang, R. Zhang, S. R. Zhang, S. S. Zhang, X. Zhang, X. P. Zhang, Yong Zhang, Yi Zhang, Y. F. Zhang, Y. L. Zhang, B. Zhao, J. Zhao, L. Zhao, L. Z. Zhao, S. P. Zhao,

F. Zheng, Y. Zheng, B. Zhou, H. Zhou, J. N. Zhou, P. Zhou, R. Zhou, X. X. Zhou, C. G. Zhu, F. R. Zhu, H. Zhu, K. J. Zhu, and X. Zuo. Ultrahigh-energy photons up to 1.4 petaelectronvolts from 12 γ-ray Galactic sources. , 594(7861):33–36, June 2021.

[38] A. U. Abeysekara, A. Albert, R. Alfaro, J. R. Angeles Camacho, J. C. Arteaga-Velázquez, K. P. Arunbabu, D. Avila Rojas, H. A. Ayala Solares, V. Baghmanyan, E. Belmont-Moreno, S. Y. BenZvi, C. Brisbois, K. S. Caballero-Mora, T. Capistrán, A. Carramiñana, S. Casanova, U. Cotti, J. Cotzomi, S. Coutiño de León, E. De la Fuente, C. de León, S. Dichiara, B. L. Dingus, M. A. DuVernois, J. C. Díaz-Vélez, R. W. Ellsworth, K. Engel, C. Espinoza, H. Fleischhack, N. Fraija, A. Galván-Gámez, D. Garcia, J. A. García-González, F. Garfias, M. M. González, J. A. Goodman, J. P. Harding, S. Hernandez, J. Hinton, B. Hona, D. Huang, F. Hueyotl-Zahuantitla, P. Hüntemeyer, A. Iriarte, A. Jardin-Blicq, V. Joshi, S. Kaufmann, D. Kieda, A. Lara, W. H. Lee, H. León Vargas, J. T. Linnemann, A. L. Longinotti, G. Luis-Raya, J. Lundeen, R. López-Coto, K. Malone, S. S. Marinelli, O. Martinez, I. Martinez-Castellanos, J. Martínez-Castro, H. Martínez-Huerta, J. A. Matthews, P. Miranda-Romagnoli, J. A. Morales-Soto, E. Moreno, M. Mostafá, A. Nayerhoda, L. Nellen, M. Newbold, M. U. Nisa, R. Noriega-Papaqui, A. Peisker, E. G. Pérez-Pérez, J. Pretz, Z. Ren, C. D. Rho, C. Rivière, D. Rosa-González, M. Rosenberg, E. Ruiz-Velasco, F. Salesa Greus, A. Sandoval, M. Schneider, H. Schoorlemmer, G. Sinnis, A. J. Smith, R. W. Springer, P. Surajbali, E. Tabachnick, M. Tanner, O. Tibolla, K. Tollefson, I. Torres, R. Torres-Escobedo, L. Villaseñor, T. Weisgarber, J. Wood, T. Yapici, H. Zhang, and H. Zhou. Multiple galactic sources with emission above 56 tev detected by hawc. *Phys. Rev. Lett.*, 124:021102, Jan 2020.

[39] H. Abdalla, F. Aharonian, F. Ait Benkhali, E. O. Angüner, C. Arcaro, C. Armand, T. Armstrong, H. Ashkar, M. Backes, V. Baghmanyan, V. Barbosa Martins, A. Barnacka, M. Barnard, Y. Becherini, D. Berge, K. Bernlöhr, B. Bi, M. Böttcher, C. Bois-

son, J. Bolmont, M. de Bony de Lavergne, M. Breuhaus, F. Brun, P. Brun, M. Bryan, M. Büchele, T. Bulik, T. Bylund, S. Caroff, A. Carosi, S. Casanova, T. Chand, S. Chandra, A. Chen, G. Cotter, M. Curyło, J. Damascene Mbarubucyeye, I. D. Davids, J. Davies, C. Deil, J. Devin, L. Dirson, A. Djannati-Ataï, A. Dmytriiev, A. Donath, V. Doroshenko, L. Dreyer, C. Duffy, J. Dyks, K. Egberts, F. Eichhorn, S. Einecke, G. Emery, J. P. Ernenwein, K. Feijen, S. Fegan, A. Fiasson, G. Fichet de Clairfontaine, G. Fontaine, S. Funk, M. Füßling, S. Gabici, Y. A. Gallant, G. Giavitto, L. Giunti, D. Glawion, J. F. Glicenstein, M. H. Grondin, J. Hahn, M. Haupt, G. Hermann, J. A. Hinton, W. Hofmann, C. Hoischen, T. L. Holch, M. Holler, M. Hörbe, D. Horns, D. Huber, M. Jamrozy, D. Jankowsky, F. Jankowsky, A. Jardin-Blicq, V. Joshi, I. Jung-Richardt, E. Kasai, M. A. Kastendieck, K. Katarzyński, U. Katz, D. Khangulyan, B. Khélifi, S. Klepser, W. Kluźniak, Nu. Komin, R. Konno, K. Kosack, D. Kostunin, M. Kreter, G. Lamanna, A. Lemière, M. Lemoine-Goumard, J. P. Lenain, F. Leuschner, C. Levy, T. Lohse, I. Lypova, J. Mackey, J. Majumdar, D. Malyshev, D. Malyshev, V. Marandon, P. Marchegiani, A. Marcowith, A. Mares, G. Martí-Devesa, R. Marx, G. Maurin, P. J. Meintjes, M. Meyer, A. Mitchell, R. Moderski, L. Mohrmann, A. Montanari, C. Moore, P. Morris, E. Moulin, J. Muller, T. Murach, K. Nakashima, A. Nayerhoda, M. de Naurois, H. Ndiyavala, J. Niemiec, L. Oakes, P. O'Brien, H. Odaka, S. Ohm, L. Olivera-Nieto, E. de Ona Wilhelmi, M. Ostrowski, S. Panny, M. Panter, R. D. Parsons, G. Peron, B. Peyaud, Q. Piel, S. Pita, V. Poireau, A. Priyana Noel, D. A. Prokhorov, H. Prokoph, G. Pühlhofer, M. Punch, A. Quirrenbach, S. Raab, R. Rauth, P. Reichherzer, A. Reimer, O. Reimer, Q. Remy, M. Renaud, F. Rieger, L. Rinchiuso, C. Romoli, G. Rowell, B. Rudak, E. Ruiz-Velasco, V. Sahakian, S. Sailer, H. Salzmann, D. A. Sanchez, A. Santangelo, M. Sasaki, M. Scalici, J. Schäfer, F. Schüssler, H. M. Schutte, U. Schwanke, M. Seglar-Arroyo, M. Senniappan, A. S. Seyffert, N. Shafi, J. N. S. Shapopi, K. Shiningayamwe, R. Simoni, A. Sinha, H. Sol, A. Specovius, S. Spencer, M. Spir-Jacob, Ł. Stawarz, L. Sun, R. Steenkamp,

C. Stegmann, S. Steinmassl, C. Steppa, T. Takahashi, T. Tavernier, A. M. Taylor, R. Terrier, J. H. E. Thiersen, D. Tiziani, M. Tluczykont, L. Tomankova, C. Trichard, M. Tsirou, R. Tuffs, Y. Uchiyama, D. J. van der Walt, C. van Eldik, C. van Rensburg, B. van Soelen, G. Vasileiadis, J. Veh, C. Venter, P. Vincent, J. Vink, H. J. Völk, Z. Wadiasingh, S. J. Wagner, J. Watson, F. Werner, R. White, A. Wierzcholska, Yu Wun Wong, A. Yusafzai, M. Zacharias, R. Zanin, D. Zargaryan, A. A. Zdziarski, A. Zech, S. J. Zhu, J. Zorn, S. Zouari, and N. Żywucka. Evidence of 100 TeV γ-ray emission from HESS J1702-420: A new PeVatron candidate. , 653:A152, September 2021.

[40] Elena Amato. The Theory of Pulsar Wind Nebulae. In *International Journal of Modern Physics Conference Series*, volume 28 of *International Journal of Modern Physics Conference Series*, page 1460160, March 2014.

[41] A. U. Abeysekara, A. Albert, R. Alfaro, C. Alvarez, J. D. Álvarez, R. Arceo, J. C. Arteaga-Velázquez, D. Avila Rojas, H. A. Ayala Solares, E. Belmont-Moreno, S. Y. BenZvi, C. Brisbois, K. S. Caballero-Mora, T. Capistrán, A. Carramiñana, S. Casanova, M. Castillo, U. Cotti, J. Cotzomi, S. Coutiño de León, C. De León, E. De la Fuente, J. C. Díaz-Vélez, S. Dichiara, B. L. Dingus, M. A. DuVernois, R. W. Ellsworth, K. Engel, C. Espinoza, K. Fang, H. Fleischhack, N. Fraija, A. Galván-Gámez, J. A. García-González, F. Garfias, A. González-Muñoz, M. M. González, J. A. Goodman, Z. Hampel-Arias, J. P. Harding, S. Hernandez, J. Hinton, B. Hona, F. Hueyotl-Zahuantitla, C. M. Hui, P. Hüntemeyer, A. Iriarte, A. Jardin-Blicq, V. Joshi, S. Kaufmann, P. Kar, G. J. Kunde, R. J. Lauer, W. H. Lee, H. León Vargas, H. Li, J. T. Linnemann, A. L. Longinotti, G. Luis-Raya, R. López-Coto, K. Malone, S. S. Marinelli, O. Martinez, I. Martinez-Castellanos, J. Martínez-Castro, J. A. Matthews, P. Miranda-Romagnoli, E. Moreno, M. Mostafá, A. Nayerhoda, L. Nellen, M. Newbold, M. U. Nisa, R. Noriega-Papaqui, J. Pretz, E. G. Pérez-Pérez, Z. Ren, C. D. Rho, C. Rivière, D. Rosa-González, M. Rosenberg, E. Ruiz-Velasco, F. Salesa Greus, A. Sandoval, M. Schneider, H. Schoor-

lemmer, M. Seglar Arroyo, G. Sinnis, A. J. Smith, R. W. Springer, P. Surajbali, I. Taboada, O. Tibolla, K. Tollefson, I. Torres, G. Vianello, L. Villaseñor, T. Weisgarber, F. Werner, S. Westerhoff, J. Wood, T. Yapici, G. Yodh, A. Zepeda, H. Zhang, and H. Zhou. Publisher Correction: Very-high-energy particle acceleration powered by the jets of the microquasar SS 433. , 564(7736):E38–E38, November 2018.

[42] Felix Aharonian, Ruizhi Yang, and Emma de Oña Wilhelmi. Massive stars as major factories of Galactic cosmic rays. *Nature Astronomy*, 3:561–567, March 2019.

[43] Andrei M. Bykov, Alexandre Marcowith, Elena Amato, Maria E. Kalyashova, J. M. Diederik Kruijssen, and Eli Waxman. High-Energy Particles and Radiation in Star-Forming Regions. , 216(3):42, April 2020.

[44] E. Parizot, A. Marcowith, E. van der Swaluw, A. M. Bykov, and V. Tatischeff. Superbubbles and energetic particles in the Galaxy. I. Collective effects of particle acceleration. , 424:747–760, September 2004.

[45] Rebecca Diesing and Damiano Caprioli. Effect of cosmic rays on the evolution and momentum deposition of supernova remnants. *Physical Review Letters*, 121(9):091101, August 2018.

[46] G. S. Bisnovatyi-Kogan and S. A. Silich. Shock-wave propagation in the nonuniform interstellar medium. *Reviews of Modern Physics*, 67:661–712, July 1995.

[47] J. P. Ostriker and C. F. McKee. Astrophysical blastwaves. *Reviews of Modern Physics*, 60:1–68, 1988.

[48] R. Bandiera and O. Petruk. Analytic solutions for the evolution of radiative supernova remnants. , 419:419–423, May 2004.

[49] D. Caprioli and A. Spitkovsky. Simulations of Ion Acceleration at Non-relativistic Shocks. III. Particle Diffusion. , 794:47, October 2014.

[50] R. Weaver, R. McCray, J. Castor, P. Shapiro, and R. Moore. Interstellar bubbles. II - Structure and evolution *[Erratum:* **220** ApJ *(1978) 742]*. *ApJ*, 218:377–395, December 1977.

[51] D. Caprioli, P. Blasi, E. Amato, and M. Vietri. Dynamical feedback of self-generated magnetic fields in cosmic ray modified shocks. *MNRAS*, 395:895–906, May 2009.

[52] D. Caprioli, E. Amato, and P. Blasi. Non-linear diffusive shock acceleration with free-escape boundary. *APh*, 33:307–311, June 2010.

[53] D. Caprioli. Cosmic-ray acceleration in supernova remnants: non-linear theory revised. *JCAP*, 7:38, July 2012.

[54] Rebecca Diesing and Damiano Caprioli. Spectrum of Electrons Accelerated in Supernova Remnants. *Physical Review Letters*, 123(7):071101, August 2019.

[55] M. A. Malkov. Analytic Solution for Nonlinear Shock Acceleration in the Bohm Limit. *Ap. J.*, 485:638–+, August 1997.

[56] M. A. Malkov, P. H. Diamond, and H. J. Völk. Critical Self-Organization of Astrophysical Shocks. *Ap. J. L.*, 533:L171–L174, April 2000.

[57] P. Blasi. A semi-analytical approach to non-linear shock acceleration. *APh*, 16:429–439, February 2002.

[58] P. Blasi. Nonlinear shock acceleration in the presence of seed particles. *APh*, 21:45–57, April 2004.

[59] E. Amato and P. Blasi. A general solution to non-linear particle acceleration at non-relativistic shock waves. *MNRAS*, 364:L76–L80, November 2005.

[60] E. Amato and P. Blasi. Non-linear particle acceleration at non-relativistic shock waves in the presence of self-generated turbulence. *MNRAS*, 371:1251–1258, September 2006.

[61] D. Caprioli and A. Spitkovsky. Simulations of Ion Acceleration at Non-relativistic Shocks: I. Acceleration Efficiency. , 783:91, March 2014.

[62] Colby C. Haggerty and Damiano Caprioli. Kinetic Simulations of Cosmic-Ray-modified Shocks. I. Hydrodynamics. , 905(1):1, December 2020.

[63] Damiano Caprioli, Colby C. Haggerty, and Pasquale Blasi. Kinetic Simulations of Cosmic-Ray-modified Shocks. II. Particle Spectra. , 905(1):2, December 2020.

[64] A. M. Bykov, A. Brandenburg, M. A. Malkov, and S. M. Osipov. Microphysics of Cosmic Ray Driven Plasma Instabilities. , May 2013.

[65] D. Caprioli and A. Spitkovsky. Simulations of Ion Acceleration at Non-relativistic Shocks: II. Magnetic Field Amplification. , 794:46, October 2014.

[66] A. Bamba, R. Yamazaki, T. Yoshida, T. Terasawa, and K. Koyama. A Spatial and Spectral Study of Nonthermal Filaments in Historical Supernova Remnants: Observational Results with Chandra. *ApJ*, 621:793–802, March 2005.

[67] M. L. Ahnen, S. Ansoldi, L. A. Antonelli, C. Arcaro, A. Babić, B. Banerjee, P. Bangale, U. Barres de Almeida, J. A. Barrio, J. Becerra González, W. Bednarek, E. Bernardini, A. Berti, W. Bhattacharyya, B. Biasuzzi, A. Biland, O. Blanch, S. Bonnefoy, G. Bonnoli, R. Carosi, A. Carosi, A. Chatterjee, M. Colak, P. Colin, E. Colombo, J. L. Contreras, J. Cortina, S. Covino, P. Cumani, P. Da Vela, F. Dazzi, A. De Angelis, B. De Lotto, E. de Oña Wilhelmi, F. Di Pierro, M. Doert, A. Domínguez, D. Dominis Prester, D. Dorner, M. Doro, S. Einecke, D. Eisenacher Glawion, D. Elsaesser, M. Engelkemeier, V. Fallah Ramazani, A. Fernández-Barral, D. Fidalgo, M. V. Fonseca, L. Font, C. Fruck, D. Galindo, R. J. García López, M. Garczarczyk, M. Gaug, P. Giammaria, N. Godinović, D. Gora, D. Guberman, D. Hadasch, A. Hahn, T. Hassan, M. Hayashida, J. Herrera, J. Hose, D. Hrupec, T. Inada, K. Ishio, Y. Konno, H. Kubo, J. Kushida, D. Kuveždić, D. Lelas, E. Lindfors, S. Lombardi, F. Longo, M. López, C. Maggio,

P. Majumdar, M. Makariev, G. Maneva, M. Manganaro, K. Mannheim, L. Maraschi, M. Mariotti, M. Martínez, D. Mazin, U. Menzel, M. Minev, R. Mirzoyan, A. Moralejo, V. Moreno, E. Moretti, V. Neustroev, A. Niedzwiecki, M. Nievas Rosillo, K. Nilsson, D. Ninci, K. Nishijima, K. Noda, L. Nogués, S. Paiano, J. Palacio, D. Paneque, R. Paoletti, J. M. Paredes, G. Pedaletti, M. Peresano, L. Perri, M. Persic, P. G. Prada Moroni, E. Prandini, I. Puljak, J. R. Garcia, I. Reichardt, W. Rhode, M. Ribó, J. Rico, C. Righi, T. Saito, K. Satalecka, S. Schroeder, T. Schweizer, S. N. Shore, J. Sitarek, I. Šnidarić, D. Sobczynska, A. Stamerra, M. Strzys, T. Surić, L. Takalo, F. Tavecchio, P. Temnikov, T. Terzić, D. Tescaro, M. Teshima, N. Torres-Albà, A. Treves, G. Vanzo, M. Vazquez Acosta, I. Vovk, J. E. Ward, M. Will, and D. Zarić. A cut-off in the TeV gamma-ray spectrum of the SNR Cassiopeia A. , 472(3):2956–2962, December 2017.

[68] R. Kulsrud and W. Pearce. Ion cyclotron resonance and cosmic ray acceleration. *The Astronomical Journal Supplement*, 73:22, February 1968.

[69] E. G. Zweibel. Energetic particle trapping by Alfven wave instabilities. In J. Arons, C. McKee, and C. Max, editors, *Particle Acceleration Mechanisms in Astrophysics*, volume 56 of *American Institute of Physics Conference Series*, pages 319–328, November 1979.

[70] J. Skilling. Cosmic ray streaming. I - Effect of Alfven waves on particles. *MNRAS*, 172:557–566, September 1975.

[71] J. Skilling. Cosmic ray streaming. II - Effect of particles on Alfven waves. *MNRAS*, 173:245–254, November 1975b.

[72] J. Skilling. Cosmic ray streaming. III - Self-consistent solutions. *MNRAS*, 173:255–269, November 1975c.

[73] P. O. Lagage and C. J. Cesarsky. Cosmic-ray shock acceleration in the presence of self-excited waves. *A&A*, 118:223–228, February 1983a.

[74] P. Blasi, E. Amato, and M. D'Angelo. High-energy cosmic ray self-confinement close to extra-galactic sources. *Physical Review Letters*, 115(12):121101, September 2015.

[75] A. Vladimirov, D. C. Ellison, and A. Bykov. Nonlinear Diffusive Shock Acceleration with Magnetic Field Amplification. , 652:1246–1258, December 2006.

[76] D. Caprioli, P. Blasi, and E. Amato. On the escape of particles from cosmic ray modified shocks. *MNRAS*, 396:2065–2073, July 2009.

[77] D. Caprioli, P. Blasi, E. Amato, and M. Vietri. Dynamical Effects of Self-Generated Magnetic Fields in Cosmic-Ray-modified Shocks. *ApJ Lett*, 679:L139–L142, June 2008.

[78] F. Giordano, M. Naumann-Godo, J. Ballet, K. Bechtol, S. Funk, J. Lande, M. N. Mazziotta, S. Rainò, T. Tanaka, O. Tibolla, and Y. Uchiyama. Fermi Large Area Telescope Detection of the Young Supernova Remnant Tycho. *ApJl*, 744:L2, January 2012.

[79] S. Archambault, A. Archer, W. Benbow, R. Bird, E. Bourbeau, M. Buchovecky, J. H. Buckley, V. Bugaev, M. Cerruti, M. P. Connolly, W. Cui, V. V. Dwarkadas, M. Errando, A. Falcone, Q. Feng, J. P. Finley, H. Fleischhack, L. Fortson, A. Furniss, S. Griffin, M. Hütten, D. Hanna, J. Holder, C. A. Johnson, P. Kaaret, P. Kar, N. Kelley-Hoskins, M. Kertzman, D. Kieda, M. Krause, S. Kumar, M. J. Lang, G. Maier, S. McArthur, A. McCann, P. Moriarty, R. Mukherjee, D. Nieto, S. O'Brien, R. A. Ong, A. N. Otte, N. Park, M. Pohl, A. Popkow, E. Pueschel, J. Quinn, K. Ragan, P. T. Reynolds, G. T. Richards, E. Roache, I. Sadeh, M. Santander, G. H. Sembroski, K. Shahinyan, P. Slane, D. Staszak, I. Telezhinsky, S. Trepanier, J. Tyler, S. P. Wakely, A. Weinstein, T. Weisgarber, P. Wilcox, A. Wilhelm, D. A. Williams, and B. Zitzer. Gamma-Ray Observations of Tycho's Supernova Remnant with VERITAS and Fermi. , 836(1):23, February 2017.

[80] L. Saha, T. Ergin, P. Majumdar, M. Bozkurt, and E. N. Ercan. Origin of gamma-ray emission in the shell of Cassiopeia A. , 563:A88, March 2014.

[81] Kohta Murase, Todd A. Thompson, Brian C. Lacki, and John F. Beacom. New class of high-energy transients from crashes of supernova ejecta with massive circumstellar material shells. *Phys. Rev. D*, 84:043003, Aug 2011.

[82] L. O'C. Drury. Escaping the accelerator; how, when and in what numbers do cosmic rays get out of supernova remnants? *ArXiv e-prints*, September 2010.

[83] D. Maurin, F. Melot, and R. Taillet. A database of charged cosmic rays. , 569:A32, September 2014.

[84] Felix A. Aharonian. Gamma rays from supernova remnants. *Astroparticle Physics*, 43:71–80, March 2013.

[85] F. Acero, A. Acharyya, R. Adam, A. Aguasca-Cabot, I. Agudo, A. Aguirre-Santaella, J. Alfaro, R. Aloisio, N. Ã lvarez Crespo, R. Alves Batista, L. Amati, E. Amato, G. Ambrosi, E.O. AngÃŒener, C. Aramo, C. Arcaro, T. Armstrong, K. Asano, Y. Ascasibar, J. Aschersleben, M. Backes, A. Baktash, C. Balazs, M. Balbo, J. Ballet, A. Baquero Larriva, V. Barbosa Martins, U. Barres de Almeida, J.A. Barrio, D. Bastieri, J.R. Baxter, J. Becker Tjus, W. Benbow, M.I. Bernardos-MartÃn, J. Bernete, A. Berti, B. Bertucci, V. Beshley, P. Bhattacharjee, S. Bhattacharyya, A. Biland, E. Bissaldi, J. Biteau, O. Blanch, P. Bordas, E. Bottacini, J. Bregeon, R. Brose, N. Bucciantini, A. Bulgarelli, M. Capasso, R.A. Capuzzo Dolcetta, P. Caraveo, M. Cardillo, R. Carosi, S. Casanova, E. Cascone, F. Cassol, F. Catalani, M. Cerruti, P. Chadwick, S. Chaty, A. Chen, M. Chernyakova, A. Chiavassa, J. Chudoba, C. Coimbra-Araujo, V. Conforti, J.L. Contreras, A. Costa, H. Costantini, P. Cristofari, R. Crocker, G. Dâ Amico, F. Dâ Ammando, A. De Angelis, V. De Caprio, E.M. de Gouveia Dal Pino, E. de Ona Wilhelmi, V. de Souza, C. Delgado, D. della Volpe, D. Depaoli, T. Di Girolamo, F. Di Pierro, R. Di Tria, L. Di Venere, S. Diebold, J.I. Djuvsland, A. Donini, M. Doro, R.d.C. Dos Anjos, V.V. Dwarkadas, S. Einecke, D. ElsÃ€sser, G. Emery, C. Evoli, D. Falceta-Goncalves, E. Fedorova, S. Fegan, G. Ferrand, E. Fiandrini, M. Filipovic, V. Fioretti, M. Fiori,

L. Foffano, G. Fontaine, S. Fukami, G. Galanti, G. Galaz, V. Gammaldi, C. Gasbarra, A. Ghalumyan, G. Ghirlanda, M. Giarrusso, G. Giavitto, N. Giglietto, F. Giordano, M. Giroletti, A. Giuliani, L. Giunti, N. Godinovic, J. Goulart Coelho, L. GrÃ©aux, D. Green, M.-H. Grondin, O. Gueta, S. Gunji, T. Hassan, M. Heller, S. HernÃ¡ndez-Cadena, J. Hinton, B. Hnatyk, R. Hnatyk, D. Hoffmann, W. Hofmann, J. Holder, D. Horan, P. Horvath, M. Hrabovsky, D. Hrupec, T. Inada, F. Incardona, S. Inoue, K. Ishio, M. Jamrozy, P. Janecek, I. JimÃ©nez MartÃnez, W. Jin, I. Jung-Richardt, J. Jurysek, P. Kaaret, V. Karas, U. Katz, D. Kerszberg, B. KhÃ©lifi, D.B. Kieda, R. Kissmann, T. Kleiner, G. Kluge, W. Kluzniak, J. KnÃ¶dlseder, Y. Kobayashi, K. Kohri, N. Komin, P. Kornecki, H. Kubo, N. La Palombara, M. LÃ¡inez, A. Lamastra, J. Lapington, M. Lemoine-Goumard, J.-P. Lenain, F. Leone, G. Leto, F. Leuschner, E. Lindfors, I. Liodakis, T. Lohse, S. Lombardi, F. Longo, R. LÃ³pez-Coto, M. LÃ³pez-Moya, A. LÃ³pez-Oramas, S. Loporchio, P.L. Luque-Escamilla, O. Macias, J. Mackey, P. Majumdar, D. Mandat, M. Manganaro, G. ManicÃ², M. Marconi, J. MartÃ, G. MartÃnez, M. Martinez, O. Martinez, A.J.T.S. Mello, S. Menchiari, D.M.-A. Meyer, S. Micanovic, D. Miceli, M. Miceli, J. Michalowski, T. Miener, J.M. Miranda, A. Mitchell, B. Mode, R. Moderski, L. Mohrmann, E. Molina, T. Montaruli, D. Morcuende, G. Morlino, A. Morselli, M. MosÃš, E. Moulin, R. Mukherjee, K. Munari, T. Murach, A. Nagai, S. Nagataki, R. Nemmen, J. Niemiec, D. Nieto, M. Nievas Rosillo, M. Nikolajuk, K. Nishijima, K. Noda, B. Novosyadlyj, S. Nozaki, M. Ohishi, S. Ohm, Y. Ohtani, A. Okumura, B. Olmi, R.A. Ong, M. Orienti, R. Orito, M. Orlandini, E. Orlando, S. Orlando, M. Ostrowski, I. Oya, F.R. Pantaleo, J.M. Paredes, B. Patricelli, M. Pecimotika, M. Peresano, J. PÃ©rez-Romero, M. Persic, O. Petruk, G. Piano, E. Pietropaolo, G. Pirola, C. Pittori, M. Pohl, G. Ponti, E. Prandini, G. Principe, C. Priyadarshi, E. Pueschel, G. PÃŒhlhofer, M.L. Pumo, A. Quirrenbach, R. Rando, S. Razzaque, P. Reichherzer, A. Reimer, O. Reimer, M. Renaud, T. Reposeur, M. RibÃ³, T. Richtler, J. Rico, F. Rieger, M. Rigoselli, L. Riitano, V. Rizi, E. Roache, P. Romano, G. Romeo,

J. Rosado, G. Rowell, B. Rudak, I. Sadeh, S. Safi-Harb, L. Saha, S. Sailer, M. SÃ¡nchez-Conde, S. Sarkar, K. Satalecka, F.G. Saturni, A. Scherer, P. SchovÃ¡nek, F. Schussler, U. Schwanke, S. Scuderi, M. Seglar-Arroyo, O. Sergijenko, M. Servillat, R.-Y. Shang, P. Sharma, H. Siejkowski, V. Sliusar, A. SÅ owikowska, H. Sol, A. Specovius, S.T. Spencer, G. Spengler, A. Stamerra, S. StaniÄ , T. Starecki, R. Starling, T. Stolarczyk, L.A. Stuani Pereira, Y. Suda, T. Suomijarvi, I. Sushch, H. Tajima, P.-H.T. Tam, S.J. Tanaka, F. Tavecchio, V. Testa, W. Tian, L. Tibaldo, D.F. Torres, N. Tothill, B. Vallage, P. Vallania, C. van Eldik, J. van Scherpenberg, J. Vandenbroucke, M. Vazquez Acosta, M. Vecchi, S. Vercellone, G. Verna, A. Viana, J. Vignatti, V. Vitale, V. Vodeb, S. Vorobiov, T. Vuillaume, S.J. Wagner, R. Walter, M. White, A. Wierzcholska, M. Will, D. Williams, L. Yang, T. Yoshida, T. Yoshikoshi, G. Zaharijas, L. Zampieri, D. Zavrtanik, M. Zavrtanik, V.I. Zhdanov, and M. ZÌ ivec. Sensitivity of the cherenkov telescope array to spectral signatures of hadronic pevatrons with application to galactic supernova remnants. *Astroparticle Physics*, 150:102850, 2023.

[86] N. Corso, R. Diesing, and D. Caprioli. Hadronic versus leptonic origin of gamma-ray emission from supernova remnants. *arXiv e-prints*, page arXiv:2301.10257, January 2023.

[87] Takahiro Sudoh and John F. Beacom. Where are Milky Way's hadronic PeVatrons? , 107(4):043002, February 2023.

Acknowledgments

The author would like to thank Damiano Caprioli, Angela V. Olinto, Raffaella Margutti, Irina Zhuravleva, and Fausto Cattaneo for their valuable feedback. The author also thanks Jordan Scherer, Cecilia Scherer-Diesing, Marcia Rimai, Daryl Diesing, Monica Rimai, Natasha Loos, and Lajos Rimai for their unwavering love and support. This research was partially supported by a William Rainey Harper Dissertation Fellowship and NSF grant AST-1909778.